Photoacoustic measurement of absolute overtone cross sections

J.H. Gutow [1], J. Davidsson [2] and R.N. Zare

Department of Chemistry, Stanford University, Stanford, CA 94305, USA

Using the photoacoustic effect, integrated absorption cross sections for the 5-0 and 6-0 C–H stretching overtones of ethane and ethylene were calibrated against the well-known cross sections for the 4-0 and 5-0 overtones of HD. The results of this calibration procedure agree well with FT-IR measurements by Quack and co-workers. Thus, these absorption cross sections would serve well as secondary reference standards in overtone measurements.

1. Introduction

Knowledge of absorption cross sections of overtone transitions is important in a number of applications that range from comparing experimental values with theoretical predictions of the mechanical and electronic anharmonicities to determining the concentration of species. Overtones are studied readily using the photoacoustic effect. Photoacoustic spectroscopy, however, does not directly yield absolute absorption cross sections, in contrast to such standard spectroscopic techniques as dual-beam and Fourier transform spectroscopy. The only practical way to measure a cross section with the photoacoustic technique is to calibrate it against a transition with a known cross section in the same frequency range. Few reference molecules are available in the visible ranges, however, because most conventional techniques lack sufficient sensitivity to measure the absolute intensity of these weak transitions.

In this Letter, we present the absolute integrated absorption cross sections, σ, for the 4-0 and 5-0 C–H stretching overtones of ethane and ethylene; σ is defined by

$$\sigma = \int_{\text{band}} \sigma(\nu)\nu^{-1}\,d\nu,$$

where $\sigma(\nu)$ is the Beer's law absorbance (log base e) at frequency ν. These absorption cross sections can be used as standards for measuring additional absorption cross sections for transitions in the same spectral region. We chose these compounds because they are readily available, behave as ideal gases, and have fairly narrow but not rotationally resolved spectroscopic features.

2. Experimental

The laser photoacoustic apparatus is an improved version of the apparatus previously used in this laboratory [1,2]. The main changes are in the design and operating conditions of the photoacoustic gas cell [3].

The photoacoustic gas cell is evacuated on a glass vacuum system pumped by an oil diffusion pump. The base pressure in this system is approximately 10^{-4} Torr. The gas mixtures for cross section calibration consist of a sample, which is ethylene (Matheson, 99.5%), ethane (Matheson, 99.0%), or propane (99.0%); a reference, HD (MSD Isotopes, >98%); and a buffer gas, xenon (Spectra Gases, >99.99%). The sample, HD, and xenon are added to the system in succession. Typical partial pressures are 1–15 Torr of sample and 100–150 Torr of HD.

---

[1] Present address: Department of Chemistry, Columbia University, New York, NY 10027, USA.

[2] Present address: Department of Physical Chemistry, Chalmers University of Technology/University of Göteborg, S-41296 Göteborg, Sweden.

Xenon is added to bring the total pressure to 300–400 Torr. Before the gas cell is sealed, the system is allowed to equilibrate for 5 min. Pressures are monitored with a Pennwalt 66-200 pressure gauge, the calibration of which was verified by comparison with an oil manometer to be accurate to approximately 0.05 Torr. To reduce interference from water absorption features, a drying agent (calcium hydride or sodium hydride powder) is kept in a finger of the cell.

The photoacoustic signal, collected by a lock-in amplifier, is recorded on a computer. The lock-in phase is set to one of the spectral features. Within a spectrum we observe no significant difference in phase between different species. This difference is a potential problem [4], however, and should be considered when using this procedure. The photoacoustic spectrum is obtained by dividing the photoacoustic signal by the relative intracavity laser power. The band integration is performed on a computer using a trapezoidal integration routine. Scans are taken slowly enough to provide approximately 10 data points within the laser bandwidth (slightly larger than 1 cm^{-1}).

3. Cross section calibration

In a mixture consisting of a reference absorber and an absorber of unknown cross section (the sample), the absolute absorption cross sections are related by

$$\frac{\sigma_u}{\sigma_r} = \frac{A_u \rho_r \nu_r}{A_r \rho_u \nu_u} . \tag{1}$$

Here the subscripts u and r refer to the sample of unknown absorption cross section and the reference sample, respectively, σ is the integrated cross section, A is the integrated area of the recorded band, ν is the band center frequency, and ρ is the density. For a nearly ideal gas, ρ is proportional to the pressure.

Eq. (1) is based on the fundamental assumption that the photoacoustic signal is proportional to the absorption coefficient convolved with the laser line profile. This assumption is true only if all the absorbed energy is rapidly thermalized, however. Vibrational overtones often satisfy this condition. For highly vibrationally excited molecules, the fluorescence rate is much slower than the rate of thermal-

ization at typical gas pressures. A significant difference in the thermalization rate of the reference and the sample can cause a phase difference in their respective photoacoustic signals.

There are other limitations to consider when choosing a reference compound. First, the absolute cross section of the reference must be well known. Second, the reference absorptions must fall in the vicinity of, but not overlap, the absorption feature of the sample. Third, the reference band must have either unresolvable structure or completely resolved lines to avoid complications from overlapping features when the band integration is performed. A fourth consideration is whether the reference compound behaves as an ideal gas and does not stick to surfaces. This feature is important in avoiding problems associated with determining the reference gas concentration.

HD is one of the few molecules that meets these criteria. The 4–0 and 5–0 HD absolute overtone cross sections are known to within 2–3% [5]. HD behaves as a nearly ideal gas and does not stick to the cell wall. Within each overtone the single rotational lines are well spaced. The multiple HD lines provide us with a number of references within a spectrum. Also, the sharp rotational features are advantageous if the HD overtones fall on top of a relatively broad absorption feature of the sample, because the HD rotational features can still be integrated accurately. The linewidth of HD, however, is less than our laser bandwidth of ≈ 1 cm^{-1}. To obtain accurate relative cross sections, the laser profile must not change significantly as the laser is scanned over an absorption feature (see Appendix). Great care has been taken to ensure this stability. From the relative intensity of the HD absorptions it is obvious when the profile of the laser line is unstable.

We have calibrated the absolute cross sections of the 5–0 and 6–0 C–H stretching overtones of ethane and ethylene and the 5–0 C–H stretching overtone of propane against the absolute cross sections of HD. Table 1 lists the measured absolute cross sections. Quack and co-workers [6] have taken FT-IR spectra of the 5–0 C–H stretching overtones of ethane and propane; their values are also shown in table 1 for comparison. Our measured absolute cross sections for the same bands are within 8% of theirs. Wong and Moore [7] have also reported an absolute cross sec-

Table 1

Frequencies and absolute cross sections of the measured C–H stretching overtones. The error bars represent 95% confidence limits based on the statistical scatter in the measurements

Compound	C–H stretching overtone	Frequency (cm^{-1})	fwhm (cm^{-1}) [a]	Cross section (fm^2) [b]	
				photoacoustic	FT-IR
ethylene	5–0	14082	102 ± 4	2.04 ± 0.14	–
	6–0	16554	136 ± 5	0.39 ± 0.04	–
ethane	5–0	13486	140 ± 3	4.08 ± 0.28	3.82
	6–0	15821	130 ± 3	0.65 ± 0.08	–
propane	5–0	13427		5.29 ± 0.20	4.84

[a] Taken from ref. [2].

[b] Note that these absolute cross sections are expressed as the observed cross section divided by the band center frequency; thus they are proportional to the formal oscillator strength of the transition. $1 \; fm^2 = 10^{-26} \; cm^2$.

tion for ethylene. Their value differs from ours by a factor of approximately 1.4. This difference is probably caused by the way they calibrated against methane, which did not properly account for their laser bandwidth.

Ethane and ethylene were chosen because they fulfill all the requirements discussed and exhibit single absorption features that are broad compared with the laser bandwidth. Because ethane and ethylene absorb at different frequencies, the hope is that one can be used as a standard that does not overlap the feature of interest. The propane data are an additional check of our procedure but are not very suitable as a reference because the features are rather broad. Typical calibration spectra of ethane and ethylene are shown in figs. 1 and 2. Note that both of these compounds have additional weak absorptions in these spectral regions. Care should be taken to account for overlap of these features when using ethane and ethylene as standards.

The absolute cross sections of overtones in the visible region have also been reported for other molecules. Various problems are associated with using each of them, however. The most useful of these molecules is methane [8]. At our resolution, however, methane exhibits partially resolved rotational structure, and many of the lines are narrower than our laser bandwidth. The most readily available compound is water [9], but it sticks to most surfaces and thereby obscures the precise partial pressure. Absolute overtone cross sections in the visible region have also been reported for acetylene [10], fluoroform [11], and HCN [12]. Their absorption cross sections are either poorly known or based on benzene. Benzene, which was calibrated against methane [13], sticks to the cell walls. Thus, for measuring integrated absorption coefficients of overtones in the visible region, we recommend use of the absolute cross sections of ethane and ethylene reported here.

Acknowledgement

Appendix

Consider two absorption features with unknown line profiles. This Appendix shows that regardless of the bandwidth of the light source, the observed ratio of the integrated cross sections is the same. The sole requirement is that the line profile of the light source does not change while scanning over any one feature.

We make the following definitions and assumptions:

(1) The laser light intensity as a function of the frequency ν is described by the function $I(\nu_0) \times L(\nu - \nu_0)$, where ν_0 is the frequency at the center of the laser profile, $I(\nu_0)$ is the integrated intensity, and $L(\nu - \nu_0)$ is the normalized laser line profile, i.e. $\int_{-\infty}^{+\infty} L(\nu - \nu_0) \, d\nu = 1$.
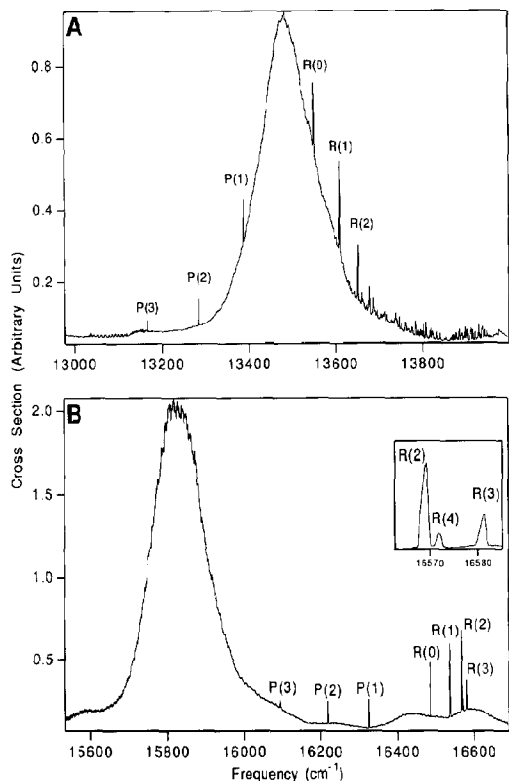
Fig. 1. Typical photoacoustic spectra of an ethane and HD mixture. The HD rotational lines are labeled. (A) shows the ethane 5–0 C–H stretch and the 4–0 HD overtone for a mixture consisting of 1.8 Torr of ethane, 117 Torr of HD, and 211.8 Torr of Xe. (B) shows the ethane 6–0 C–H stretch and the 5–0 HD overtone for a mixture consisting of 8.7 Torr of ethane, 125.2 Torr of HD, and 229 Torr of Xe. Note the additional weak ethane band in the region 16300 to 16700 cm^{-1}. The inset shows details of the HD R-branch bandhead.

(2) The band absorption profile is described by the function $B_i(\nu)$, where $i=1$ or 2. We also assume that $\int_{-\infty}^{+\infty} B_i(\nu) \, d\nu$ is finite.

The observed band profile as the laser is scanned is

$$\int_{-\infty}^{+\infty} B_i(\nu) I(\nu_0) L(\nu - \nu_0) \, d\nu$$

$$= I(\nu_0) \int_{-\infty}^{+\infty} B_i(\nu) L(\nu - \nu_0) \, d\nu. \qquad (A.1)$$

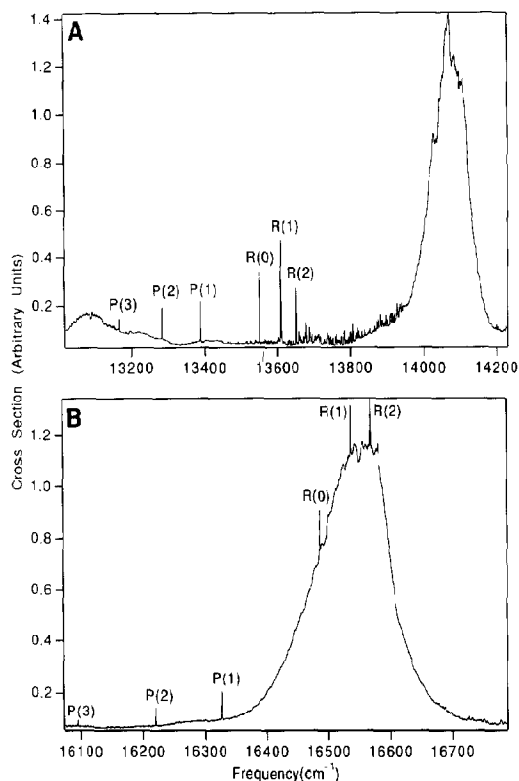Dividing eq. (A.1) by the integrated intensity $I(\nu_0)$,

Fig. 2. Typical photoacoustic spectra of an ethylene and HD mixture. The HD rotational lines are labeled. (A) shows the ethylene 5–0 C–H stretch and the 4–0 HD overtone for a mixture consisting of 2.3 Torr of ethylene, 109.7 Torr of HD, and 202.7 Torr of Xe. Note the weak ethylene band below 13300 cm^{-1}. (B) shows the ethylene 6–0 C–H stretch and the 5–0 HD overtone for a mixture consisting of 10.8 Torr of ethylene, 152.8 Torr of HD, and 263.5 Torr of Xe.

we obtain the intensity-independent profile $\int_{-\infty}^{+\infty} B_i(\nu) L(\nu - \nu_0) \, d\nu$. The integrated area of the observed band profile i is obtained by integrating over ν_0,

$$A_i = \int_{-\infty}^{+\infty} \int_{-\infty}^{+\infty} B_i(\nu) L(\nu - \nu_0) \, d\nu \, d\nu_0. \qquad (A.2)$$

Since the convolution $\int_{-\infty}^{+\infty} B_i(\nu) L(\nu - \nu_0) \, d\nu$ converges uniformly to a continuous function, i.e. the observed profile exists, we may change the order of integration [13]. Hence A_i may also be written as

$$A_i = \int_{-\infty}^{+\infty} B_i(\nu) \int_{-\infty}^{+\infty} L(\nu - \nu_0) \, d\nu_0 \, d\nu. \qquad (A.3)$$

We can apply the transform $\nu = x$ and $\nu_0 = x - y$ to eq. (A.3). The Jacobian of this transform is -1. So, adjusting the limits properly,

$$A_i = \int_{-\infty}^{+\infty} B_i(x) \int_{-\infty}^{+\infty} L(y)\, \mathrm{d}y\, \mathrm{d}x$$

$$= \int_{-\infty}^{+\infty} B_i(x)\, \mathrm{d}x \int_{-\infty}^{+\infty} L(y)\, \mathrm{d}y$$

$$= \int_{-\infty}^{+\infty} B_i(x)\, \mathrm{d}x, \qquad (A.4)$$

where we have used the normalization property of the laser profile function. Thus,

$$\frac{A_1}{A_2} = \frac{\int_{-\infty}^{+\infty} B_1(x)\, \mathrm{d}x}{\int_{-\infty}^{+\infty} B_2(x)\, \mathrm{d}x}, \qquad (A.5)$$

which is the ratio of the integrated areas.

References

[1] D.W. Chander, W.E. Farneth and R.N. Zare, J. Chem. Phys. 77 (1982) 4447.

[2] M.W. Crofton, C.G. Stevens, D. Klenerman, J.H. Gutow and R.N. Zare, J. Chem. Phys. 89 (1988) 7100.

[3] J. Davidsson, J.H. Gutow and R.N. Zare, J. Phys. Chem. 94 (1990) 4069.

[4] V.P. Zharov and V.S. Letokhov, in: Springer series in optical sciences, Vol. 37. Optoacoustic spectroscopy, ed. T. Tasmir (Springer, Berlin, 1986).

[5] J.T. Trauger and M.E. Mickelson, Icarus 56 (1983) 176.

[6] M. Quack, private communication.

[7] J.S. Wong and C.B. Moore, J. Chem. Phys. 77 (1982) 603.

[8] L.P. Giver, J. Quant. Spectry. Radiative Transfer 19 (1978) 311.

[9] J.Y. Mandin, J.P. Chevillard, C. Camy-Peyret and J.M. Falud, J. Mol. Spectry. 116 (1986) 167.

[10] K.K. Lehmann, J. Chem. Phys. 91 (1989) 2759.

[11] J. Segall, R.N. Zare, H.R. Dübal, M. Lewerenz and M. Quack, J. Chem. Phys. 86 (1987) 634.

[12] A.M. Smith, U.G. Jørgensen and K.K. Lehmann, J. Chem. Phys. 87 (1987) 5649.

[13] K.V. Reddy, D.F. Heller and M.J. Berry, J. Chem. Phys. 76 (1982) 2814.

[14] J.C. Amizago and L.A. Rubenfeld, Advanced calculus (Wiley, New York, 1980) pp. 243ff.